

Structural control of vertically aligned multiwalled carbon nanotubes by radio-frequency plasmas

Jitendra Menda, Benjamin Ulmen, Lakshman K. Vanga,
Vijaya K. Kayastha, and Yoke Khin Yap^{a)}

Department of Physics, Michigan Technological University, Houghton, Michigan 49931

Zhengwei Pan, Iliia N. Ivanov, Alex A. Puzetky, and David B. Geohegan

*Condensed Matter Sciences Division, Oak Ridge National Laboratory, Oak Ridge, Tennessee 37831-6056
and Department of Materials Science and Engineering, University of Tennessee, Knoxville, Tennessee 37996*

(Received 18 May 2005; accepted 27 August 2005; published online 18 October 2005)

Plasma-enhanced chemical vapor deposition is the only technique for growing individual vertically aligned multiwalled carbon nanotubes (VA-MWCNTs) at desired locations. Inferior graphitic order has been a long-standing issue that has prevented realistic applications of these VA-MWCNTs. Previously, these VA-MWCNTs were grown by a one-plasma approach. Here, we demonstrate the capability of controlling graphitic order and diameters of VA-MWCNTs by decoupling the functions of the conventional single plasma into a dual-plasma configuration. Our results indicate that the ionic flux and kinetic energy of the growth species are important for improving graphitic order of VA-MWCNTs. © 2005 American Institute of Physics. [DOI: 10.1063/1.2115068]

Carbon nanotubes (CNTs) are among the important materials for the advancement of future nanoscience and nanotechnology. Recently, vertically aligned multiwalled carbon nanotubes (VA-MWCNTs) have gained additional attention for innovative applications, such as nanotubes antennas,¹ vertical transistors,^{2,3} and vertical biosensors.⁴ Ideally, these applications require VA-MWCNTs to be grown at desired patterns. Plasma-enhanced chemical vapor deposition (PECVD) is the only technique for growing individual VA-MWCNTs at desired locations. However, the graphitic order of these VA-MWCNTs is inferior to the multiwall CNTs grown by arc discharge⁵ and thermal chemical vapor deposition.^{6–8} This has been a long-standing issue for realistic uses of VA-MWCNTs in applications, such as electron field emission devices.^{9–13}

VA-MWCNTs grown by PECVD are usually called carbon nanofibers (CNFs) and have highly distorted structures. Previously, these CNFs were grown by a one-plasma approach.^{14–17} Here, we found that the graphitic order and diameters of VA-MWCNTs are controllable by decoupling the functions of single plasma into a dual-plasma configuration. Our results indicate that the ionic flux and kinetic energy of the growth species are important for improving the graphitic order of VA-MWCNTs.

By a dual-radio-frequency (rf) PECVD technique (dual-rf-PECVD), we shown that VA-MWCNTs can be grown to an area as of 25 cm² at substrate temperatures as low as 540 °C.¹⁸ The dual-rf-PECVD system has a pair of parallel electrodes. The plasma produced on the top and the bottom electrodes is referred as the top plasma and the bottom plasma, respectively. The spacing between the two electrodes is 5 cm with the substrate located 3.5 cm from the top electrode. This substrate is placed on a heater and electrically contacted with the bottom electrode. The heater controls the growth temperatures by using a proportional-integration-differentiation system.

The top plasma ionizes the hydrocarbon gas and determines the ionic density of the growth species. This ionic density is controlled by the forward power of a rf generator. Another rf power generator produces the bottom plasma and induces bias voltages on the substrates and the bottom electrode. This bias voltage will accelerate the ionic species to bombard the growth surface and control their kinetic energy.

Ni films were used as the catalyst for growing VA-MWCNTs. These films are deposited by pulsed laser deposition on Si substrates that have a layer of SiO₂ film (~500 nm). Before the growth of MWCNTs, these Ni films were heat treated at 600 °C for 10 min. Methane gas (CH₄, 99.9%) flowed at a rate of 350 sccm and resulted in a constant pressure of 0.2 mTorr. The two rf plasmas were then generated to initiate the growth of MWCNTs at 600 °C. We chose to use thick Ni films (25 nm) for growing thick MWCNTs to enable easier detection of diameter changes of the MWCNTs.

We have investigated the effect of the top plasma while keeping the substrate biasing at -150 V. As shown in Fig. 1, the diameters of the MWCNTs increased accordingly with the increase in the forward power (50 W to 200 W) to the top plasma. The increase in this power enhances the ionic density inside the top plasma. Plasma heating will increase the surface-free energy (ΔE_S , in energy per unit area) of the Ni nanoparticles on the adjacent substrates. The total free energy of a cluster can be expressed as $\Delta E = \Delta E_S A + \Delta E_V V$, where ΔE_V is the volume-free energy (in energy per unit volume), and A and V are the surface area and the volume of

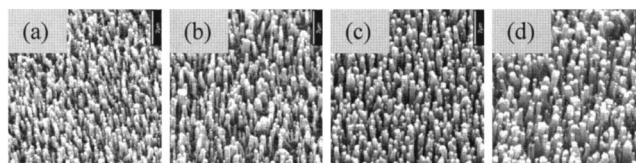


FIG. 1. Scanning electron microscope (SEM) images of VA-MWCNTs grown at different top plasma forward powers: (a) 50 W, (b) 100 W, (c) 150 W, and (d) 200 W. The substrate biasing is maintained at -150 V for all cases. Scale bar=2 μm .

^{a)} Author to whom correspondence should be addressed; electronic mail: ykyap@mtu.edu

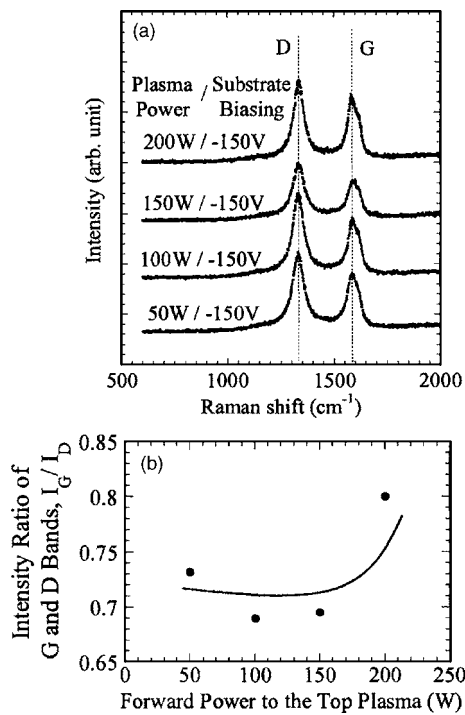


FIG. 2. (a) Raman spectra for VA-MWCNTs grown at various top plasma forward power and (b) the corresponding I_G/I_D relation.

the cluster, respectively.¹⁹ At stable mode, ΔE_S is positive while ΔE_V is negative in value. As plasma heating increases the surface-free energy ΔE_S , smaller catalyst particles will diffuse and merge as larger clusters. This will decrease A and increase V . Thus, the volume-free energy (ΔE_V) term will dominate and minimize the total-free energy (ΔE becomes more negative). The formation of large particles will result in the growth of VA-MWCNTs with larger diameters.

We use Raman spectroscopy to examine the graphitic order of these VA-MWCNTs. This is done by comparing the intensity of the graphitic (G) and disordered (D) Raman bands. The G and D bands represent the zone center phonons of E_{2g} symmetry and the K -point phonons of A_{1g} symmetry, respectively.²⁰ The intensity ratio of these two bands (I_G/I_D) is commonly used as a measure of graphitic order of carbon-based materials. All measurements are carried out by a confocal micro-Raman system, using a HeNe excitation laser ($\lambda=632.8$ nm). The Raman spectra for MWCNTs samples grown by various top plasma forward power are shown in Fig. 2(a). The relation of I_G/I_D to the forward power is shown in Fig. 2(b). As shown, the I_G/I_D ratio increases at a forward power of 200 W, which indicates the enhancement of graphitic order of the VA-MWCNTs.

We have then investigated the effect of the bottom plasma by varying the negative dc substrate bias voltage while keeping the top plasma forward power at 200 W. As shown in Fig. 3, an increase in the diameter of the tube is

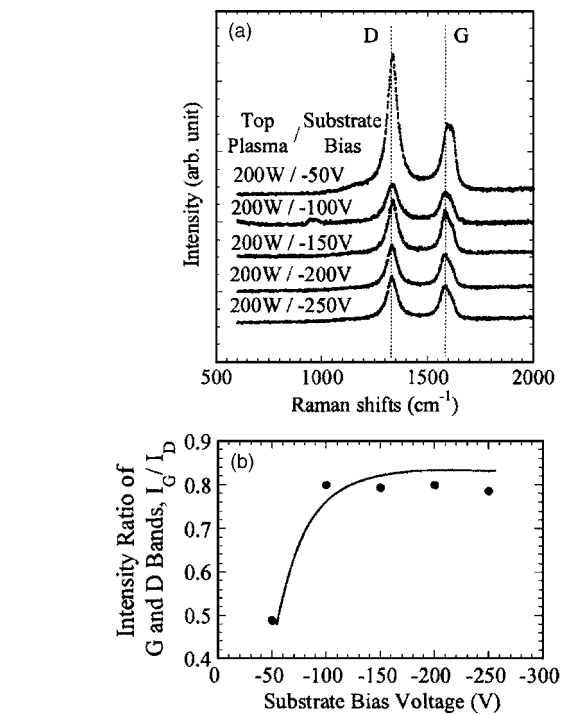


FIG. 4. (a) Raman spectra for VA-MWCNTs grown at various substrate biasing and (b) the corresponding I_G/I_D relation.

observed when the biasing varied from [Fig. 3(a)] -50 V, [Fig. 3(b)] -100 V, to [Fig. 3(c)] -150 V. The increase in substrate biasing enhanced the kinetic energy of the impinging ions. The ionic flux near the substrate region will also be increased. Thus, the energy transfer to the substrate surface will be enhanced through ion bombardment. This will increase the surface energy of the Ni nanoparticles and induce larger Ni clusters, as discussed earlier. Thus, the diameters of the MWCNTs increased. However, when the bias voltage reaches a level between -150 and -200 V [Figs. 3(c) and 3(d)], a decrease in the diameters of the MWCNTs is detected. This can be explained by the sputtering of Ni nanoparticles by the energetic ions. The diameters of MWCNTs continue to decrease at a biasing of -250 V [Fig. 3(e)]. No MWCNTs were formed when the biasing is higher than -350 V, which is the total re-sputtering region.

Figure 4(a) shows the Raman spectra for these VA-MWCNTs. The corresponding relation of I_G/I_D to the substrate biasing is shown in Fig. 4(b). As shown, the I_G/I_D ratio is low (~ 0.48) at low substrate biasing (-50 V), but is increased to I_G/I_D of ~ 0.80 at higher substrate biasing. This result indicates that a biasing threshold occurred (between -50 to -100 V) for growing MWCNTs with high graphitic order. These are consistent with the obtained transmission electron microscope (TEM) images shown in Fig. 5. At a biasing of [Fig. 5(a)] -50 V, the structure of MWCNTs are highly distorted. Defects/debris at the sidewalls are clearly

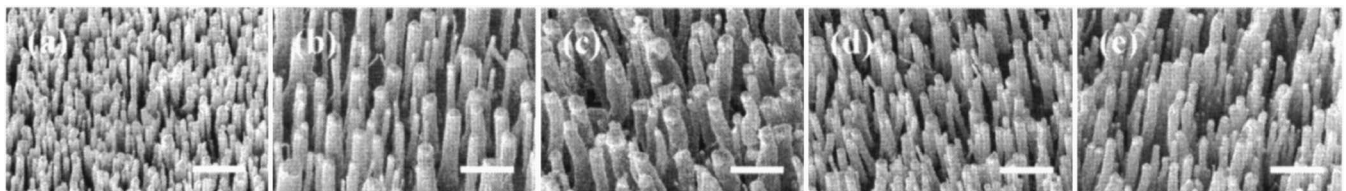


FIG. 3. SEM images of VA-MWCNTs grown at different substrate biasing: (a) -50 V, (b) -100 V, (c) -150 V, (d) -200 V, and (e) -250 V. The top plasma forward power is maintained at 200 W for all cases. Scale bar = $1 \mu\text{m}$.

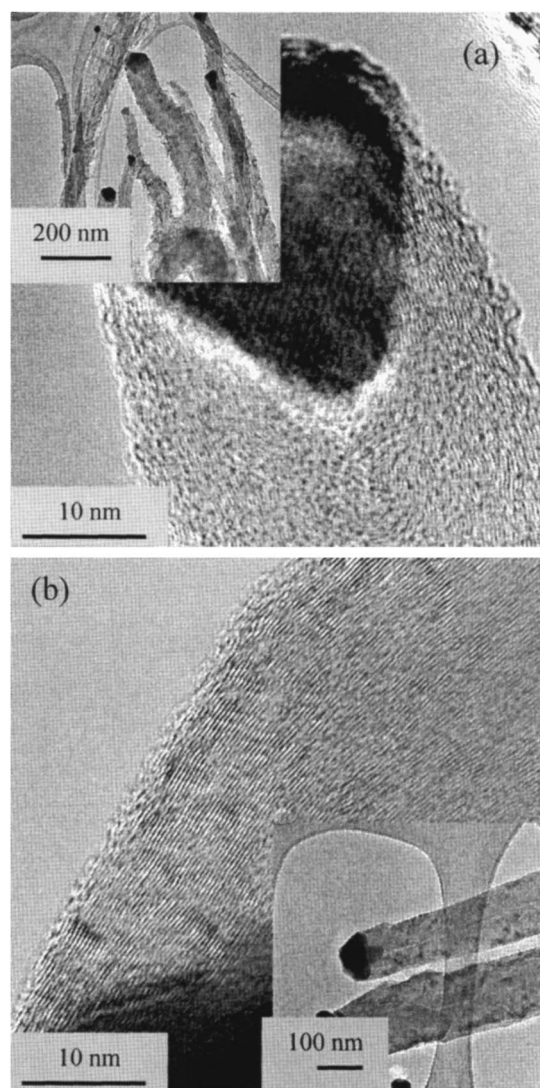


FIG. 5. TEM images of MWCNTs grown a substrate biasing of (a) -50 V and (b) -150 V. The top plasma forward power is maintained at 200 W for both cases.

shown in the inset. At higher biasing (-150 V), MWCNTs with higher graphitic order are grown as shown in Fig. 5(b). These MWCNTs have straighter and smoother sidewalls as shown in the inset. This result indicates that the growth species with a high kinetic energy is important for the formation of MWCNTs with improved graphitic order. We believe that high substrate biasing will generate directional ion flux and promote covalent bonds of carbon along the tubular axis, as we proposed previously.¹⁸ Our results are consistent with the theory that both the kinetic energy (E_k) and the potential energy (U) of the growth species are contributing to the structural properties of solids.²¹ Structural orders of MWCNTs will be enhanced when the total energy ($E = E_k + U$) of the growth species well exceeds the cohesive energy (E_c) of the sp^2 -bonded carbon networks (~ 7.4 eV/atom). The exceeding energy ($E - E_c$) will be quenched to produce atomic scale heating²¹ that promotes atomic diffusion and enhances the structural order of VA-MWCNTs. As guided by these findings, we have then optimized the growth of VA-MWCNTs at thinner catalyst films. For example, at 200 W of top plasma and substrate biasing of -100 V, straight VA-MWCNTs with uniform diameter (~ 60 nm) are grown at 450 °C as shown in Fig. 6.

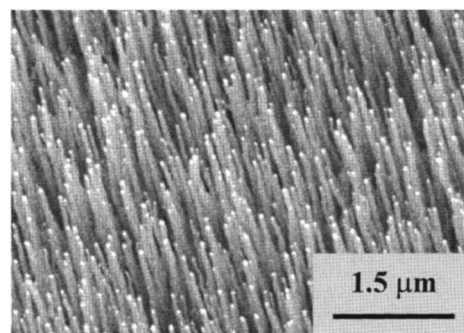


FIG. 6. SEM images of straight VA-MWCNTs at optimum growth conditions.

In summary, the diameters and graphitic order of VA-MWCNTs can be effectively controlled by the dual-rf-PECVD technique. This is accomplished by adjusting the ionic flux and the negative dc bias voltages on the substrates independently by a dual-rf-plasma approach.

One of the authors (Y.K.Y.) acknowledges support from the Michigan Tech Research Excellence Fund, the Department of the Army (Grant No. W911NF-04-1-0029, through the City College of New York), and the Center for Nanophase Materials Sciences sponsored by the Division of Materials Sciences and Engineering, U.S. Department of Energy, under Contract No. DE-AC05-00OR22725 with UT-Battelle, LLC.

¹Y. Wang, K. Kempa, B. Kimball, J. B. Carlson, G. Benham, W. Z. Li, T. Kempa, J. Rybczynski, A. Herczynski, and Z. F. Ren, *Appl. Phys. Lett.* **85**, 2067 (2004).

²J. Li, R. Stevens, L. Delzeit, H. T. Ng, A. Cassell, J. Han, and M. Meyyappan, *Appl. Phys. Lett.* **81**, 910 (2002).

³A. M. Cassell, J. Li, R. M. D. Stevens, J. E. Koehne, L. Delzeit, H. T. Ng, Q. Ye, J. Han, and M. Meyyappan, *Appl. Phys. Lett.* **85**, 2364 (2004).

⁴C. V. Nguyen, L. Delzeit, A. M. Cassell, J. Li, J. Han, and M. Meyyappan, *Nano Lett.* **2**, 1079 (2002).

⁵S. Iijima, *Nature (London)* **354**, 56 (1991).

⁶W. Z. Li, S. S. Xie, L. X. Qian, B. H. Chang, B. S. Zou, W. Y. Zhou, R. A. Zhao, and G. Wang, *Science* **274**, 1701 (1996).

⁷R. Kamalakaran, M. Terrones, T. Seeger, P. Kohler-Redlich, and M. Rühle, Y. A. Kim, T. Hayashi, and M. Endo, *Appl. Phys. Lett.* **77**, 3385 (2000).

⁸V. K. Kayastha, Y. K. Yap, Z. Pan, I. N. Ivanov, A. A. Puzosky, and D. B. Geohegan, *Appl. Phys. Lett.* **86**, 253105 (2005).

⁹A. G. Rinzler, J. H. Hafner, P. Nikolaev, L. Lou, S. G. Kim, D. Tománek, P. Nordlander, D. T. Colbert, and R. E. Smalley, *Science* **269**, 1550 (1995).

¹⁰W. A. de Heer, D. T. Chátelain, and D. Ugarte, *Science* **270**, 1179 (1995).

¹¹N. de Jonge, Y. Lamy, K. Schroots, and T. H. Oosterkamp, *Nature (London)* **420**, 393 (2002).

¹²Y. Wei, C. Xie, K. A. Dean, and B. F. Coll, *Appl. Phys. Lett.* **79**, 4527 (2001).

¹³J.-M. Bonard, C. Klinker, K. A. Dean, and B. F. Coll, *Phys. Rev. B* **67**, 115406 (2003).

¹⁴Z. F. Ren, Z. P. Huang, J. W. Xu, J. H. Wang, P. Bush, M. P. Siegal, and P. N. Provencio, *Science* **282**, 1105 (1998).

¹⁵C. Bower, W. Zhu, S. Jin, and O. Zhou, *Appl. Phys. Lett.* **76**, 1776 (2000).

¹⁶M. Chhowalla, K. Teo, C. Ducati, N. Rupasinghe, G. Amaratunga, A. Ferrari, D. Roy, J. Robertson, and W. Milne, *J. Appl. Phys.* **90**, 5308 (2001).

¹⁷A. V. Melechko, V. I. Merkulov, T. E. McKnight, M. A. Guillorn, K. L. Klein, D. H. Lowndes, and M. L. Simpson, *J. Appl. Phys.* **97**, 41301 (2005).

¹⁸T. Hirao, K. Ito, H. Furuta, Y. K. Yap, T. Ikuno, S. Honda, Y. Mori, T. Sasaki, and K. Oura, *Jpn. J. Appl. Phys., Part 2* **40**, L631 (2001).

¹⁹L. E. Brus, J. A. W. Harkless, and F. H. Stillinger, *J. Am. Chem. Soc.* **118**, 4834 (1991).

²⁰Y. K. Yap, M. Yoshimura, Y. Mori, and T. Sasaki, *Appl. Phys. Lett.* **80**, 2559 (2002).

²¹A. Anders, *Appl. Phys. Lett.* **80**, 1100 (2002).